Effect of Fin-Shaped Electrodes on Flow Mixing and Pressure Drop in an Electroosmotic Micromixer

Bahrami, Dariush; Bayareh, Morteza*[+]

Department of Mechanical Engineering, Shahrekord University, Shahrekord, I.R. IRAN

Usefian, Azam

Department of Electrical Engineering, École de Technologie Supérieure (ÉTS), CANADA

ABSTRACT: *Production of a homogeneous solution is of great interest for Lab-on-a-Chip (LOC) applications. Since the fluid flow in microchannels is laminar, the LOC devices have low mixing efficiency in passive mixers. The present study proposes a novel electroosmotic micromixer in which the electrodes have a fin-shaped structure in the mixing chamber. In other words, the combined effect of obstacle and electro-osmosis is evaluated. The effect of various parameters such as electrode angle, electrode height, inlet velocity, alternating current, and frequency on mixing index and pressure drop is investigated. Vortices are formed around the electrodes due to the applied electric field and their fin-shaped structure. It is revealed that the mixing index is an increasing function of applied voltage. The results demonstrate that there is an optimal value for the parameters, including frequency, electrode height, inlet velocity, and electrode angle. An increase in the mixing efficiency is accompanied by an enhancement in the pressure drop. It is revealed that the maximum efficiency is achieved when the electrode height is 5 μm and the electrode angle is 60°. The coefficient of performance of the proposed micromixer is more than that of the reference mixer when the electrode height is 2.5 μm and the electrode angle is 90°.*

KEYWORDS: *Lab-on-a-chip; Electroosmotic micromixer; Mixing efficiency; Pressure drop; COP.*

INTRODUCTION

Microfluidic LOC technologies have attracted the attention of many researchers due to their wide applications, including biomedical, chemistry systems, DNA sequencing, and cancer cell diagnostic [1, 2]. Micromixer is one of the most important branches of LOC, in which the mixing process of two or more fluids occurs. Micromixers are divided into active and passive ones [3, 4]. In passive mixers, complex geometry should be employed to reach high mixing quality [5]. This is due to that the Reynolds number is low in microfluidic devices and if a simple structure is used, the mixing process is performed as a result of the diffusion mechanism. Serpentine [6, 7], Zigzag [8], spiral [9, 10] micromixers were employed to improve the mixing index of Newtonian and non-Newtonian fluids. For example, *Chen et al.* [6] introduced square-wave, multi-wave, and zigzag micromixers and demonstrated that mixing index is reduced with the Reynolds number for $0.1 < Re < 1$ and

***** *To whom correspondence should be addressed.*
+ *E-mail: m.bayareh@sku.ac.ir*
1021-9986/2023/1/208-221 14/$/6.04

is enhanced with Re changing from 1 to 100. A novel spiral micromixer with sinusoidal channel walls was utilized by *Bahrami* and *Bayareh* [10] to intensify the mixing process for 1 < Re < 100 numerically and experimentally. They reached a mixing efficiency of 99.11% and reported that the maximum mixing degree is obtained for optimal values of amplitude and wavelength. Although the mixing index reaches even about 100%, the time for complete mixing is relatively high. Besides, as the mixing quality is improved, the mixing length enhances. In an active micromixer, an external force causes laminar layers to break and makes it chaotic to mix the fluids. The external force is induced by an acoustic wave, magnetic field, or electric field. For instance, *Hejazian* and *Nguyen* [11] utilized magnetofluidic actuation to mix a diluted ferrofluid and non-magnetic flow in a straight microchannel for volume flow rates ranging from 20 to 300 μL/min. They showed that the micromixing degree is determined by the competition between the secondary flow created due to the magnetic field and the pressure-driven flow. *Lim et al.* [12] considered a droplet acoustofluidic system to examine the impact of transducer geometry on micromixing and demonstrated that the acoustic streamings that are generated due to external sound filed to improve the mixing quality by 25% and 43% for concave and convex transducers. To mix high-conductivity solutions, *Lv* and *Chen* [13] proposed a novel hybrid microdevice based on electric heating and an external heat source. They revealed that the electrode and heat source affect the solution when a film heater is mounted at the bottom of the channel.

Electroosmotic-driven micromixers have been considered in many numerical and experimental investigations due to their low mixing time [14-20]. *Khakpour* and *Ramiar* [21] performed numerical simulations to investigate electrode arrangement and the shape of the chamber in an electroosmotic micromixer. They demonstrated that raising the electrodes increases the mixing degree and decreases the velocity. They reported that the use of a circular chamber leads to a mixing efficiency of 99% when thinlet velocity is 64 μm/s. *Seo et al.* [22] simulated a ring-type electroosmotic micromixer with different obstacle configurations. Four electrodes were employed to produce Alternating Current (AC) in their microchannel. Their results showed that the mixing index is approximately the same for circular and rectangular obstacles. *Usefian et al.* [23] investigated a ring-type electroosmotic micromixer with a rotating cylinder inside the mixing chamber using the finite element method for solving non-linear equations. They revealed that an increase in the cylinder angular velocity from 0.0148 to 1.148 results in mixing enhancement by 26.65%. Besides, the mixing efficiency of non-Newtonian liquids was found to be 20.61% higher than that of Newtonian ones. *Basati et al.* [24] studied electroosmotic flow in a microchannel by utilizing the Lattice Boltzmann method. They compared four types of microchannels, including the smooth wall, diverged wall, converged wall, and converged-diverged wall, and found that maximum and minimum mixing quality corresponds to the converged and diverged microchannels, respectively. *Zhang et al.* [25] conducted an effective Y-shaped electroosmotic micromixer to evaluate the effect of parameters such as inlet velocity, alternating current, and frequency. They reached the mixing efficiency of 94.7% for V=14 V, f=400 Hz, and u=1500 μm/s. *Alipanahrostami* and *Ramiar* [26] used AC and DC to design an efficient electroosmotic micromixer. Their result revealed a 23% improvement for AC compared to DC. They also considered the blood as a non-Newtonian fluid and found that their proposed micromixer has high performance for mixing Newtonian and non-Newtonian fluids. *Usefian* and *Bayareh* [27] analyzed a novel electroosmotic micromixer experimentally and numerically and showed that vortex generation leads to mixing improvement. An optimum distance between two electrodes was determined to achieve maximum mixing efficiency. Besides, it was demonstrated that an increase in voltage from 0 to 40 V leads to an enhancement in the mixing index by 74.56%.

The effects of Reynolds number and non-Newtonian fluid on the mixing process in an electroosmotic micromixer were studied by *Hadigol et al.* [28]. They showed that an increase in Reynolds number leads to a reduction in the mixing index. Furthermore, their proposed micromixer was more efficient for non-Newtonian fluids in comparison with the Newtonian ones. *Jalili et al.* [29] investigated a ring-type electroosmotic micromixer numerically using COMSOL-Multiphysics software. Three different obstacles, including circle, square, and rhombus were studied for various inlet velocities. They reported that the shape of obstacles does not have a significant effect on the mixing process. Also, the mixing efficiency is a decreasing function of the inlet velocity.

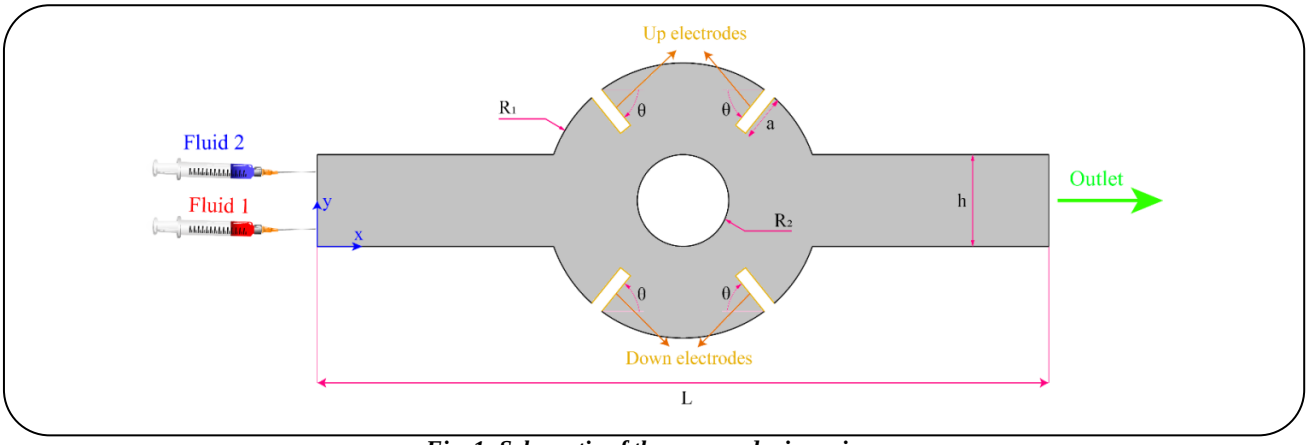

Fig. 1: Schematic of the proposed micromixer.

In a numerical study, *Chen et al.* [30] examined the effects of the number and array of electrodes in a two-dimensional serpentine electroosmotic micromixer. Their results revealed that the number and array of electrodes have a substantial effect on the mixing index and the micromixer with three pairs of electrodes improves the mixing index by 98.2%. This value was 30% more than that of an electrodeless micromixer. *Zhou et al.* [31] proposed an effectual ring-type electroosmotic micromixer by changing geometrical parameters. A rib was located in the center of the base microchannel. They used a combination of rectangular and circular ribs and placed negative and positive electrodes on them. They reported that as the voltage increases and inlet velocity decreases, the mixing quality is improved. *Shamloo et al.* [32] presented a ring-type electro-osmotic micromixer and studied the effect of inlet velocity, voltage, frequency, and phase of AC. They used diamond geometry for the outer ring and observed a 1.4% decrement in the mixing index. They also combined two circular rings and obtained an increase in the mixing index by 0.4% compared to one ring-type micromixer. *Chen* and *Wu* [33] designed a novel electroosmotic micromixer with different arrangements of electrodes numerically. They considered a serpentine micromixer with three pairs of electrodes and reached a mixing index of 98.2% for voltage of 10 V and frequently of 16 Hz.

According to the literature, the location of electrodes has a crucial role in the mixing process. The previous works confirmed that the mixing improvement is attained when the pressure drop is enhanced. Hence, these two parameters should be determined to optimize the performance of a micromixer. The main innovations of the present work are as follows: (i) a ring-type electroosmotic micromixer is considered in which four thick electrodes are placed inside the mixing chamber as obstacles. In other words, the combined effect of obstacle and electro-osmosis is evaluated in this work. To the best of the authors' knowledge, the proposed geometry has not been considered for electro-osmotic micromixers. (ii) The effect of angle and height of electrodes on mixing efficiency and pressure drop is investigated. Hence, the location of electrodes relative to the inlet flow is changed, leading to the change in size and position of vortices formed in the mixing chamber. Fig. 1 shows the geometry of the present work. Four AC electrodes with a specific height, a, are placed inside the mixing chamber. The micromixer with a = 0 is considered as the reference mixer. The dimensions of the micromixer are given in Table 1. Since the inlet flow enters the microchannel using a syringe pump, the inlet flow rate is adjustable.

THEORETICAL SECTION

Governing equations

To simulate the electroosmotic micromixing, the flow field is simulated by solving continuity and Navier-Stokes equations. The electric field and concentration one are also solved by Laplace and convection-diffusion equations, respectively. The boundary conditions are given in Table 2.

Flow field

The continuity and Navier-Stokes equations for a two-dimensional Newtonian incompressible flow are as follows [23, 32]:

$$\nabla.\vec{u} = 0 \tag{1}$$

$$\rho\frac{D\vec{u}}{Dt} = -\nabla p + \mu\nabla^2\vec{u} + \rho_e\vec{E} \tag{2}$$

Table 1: Dimensions of the proposed micromixer.

Parameter	Value
L (μm)	80
h (μm)	10
a (μm)	0-7.5
R_1 (μm)	15
R_2 (μm)	5
θ (degree)	0-90

Table 2: Boundary conditions employed for the present simulations.

Physical modeling	Boundary conditions
Flow field	Fully developed flow at the inlet, u = U_{in}. Slip velocity boundary condition on walls, $u \neq 0$. Atmosphere pressure at outlet, P = 0 Pa.
Electric field	Insulated wall for all the boundaries, $-\sigma\nabla V \times n = 0$. Sinusoidal boundary condition on electrodes, $V = V_o\, Sin(2\pi f t + E_o)$.
Concentration field	C = 1 mol/m^3 at the upper-half inlet C = 0 mol/m^3 at the lower-half inlet Convection at the outlet.

Where $\vec{u}$ is the velocity vector, p the pressure, ρ the density, μ the fluid viscosity, $\vec{E}$ the electric field strength, and ρ_e the net charge density, which is non-zero only in the electrical double layer. The electroosmotic slip velocity is used for all walls and thus, the term $\rho_e\vec{E}$ can be neglected in the momentum equation. In other words, when this boundary condition is applied, the electroosmotic flow is created, leading to that the liquid being displaced in the electric double layer. Thus, a force is imposed on the solution in the vicinity of the wall, resulting in the fluid flows in the direction of the electric field. Besides, the flow is assumed to be fully developed at the channel inlet and no normal stress is applied to the channel outlet.

Electric field

The electric potential V_e is applied to the fluid chamber and is calculated by using the following Laplace equation:

$$\nabla^2 \mathrm{V_e} = 0 \tag{3}$$

Where $\vec{E} = -\nabla V_e$. The applied voltage is AC:

$$\mathrm{V} = \mathrm{V_o}\,\mathrm{Sin}(2\pi \mathrm{ft} + \mathrm{E_o}) \tag{4}$$

WWhere f is the frequency. It should be noted that all the space inside the microchannel, except for the electrode areas, is electrically insulated.

Concentration field

The concentration field of the electrolyte solution or any other chemical liquid is:

$$\nabla.(-\mathrm{D}\nabla \mathrm{C}) = \mathrm{R} - \vec{\mathrm{u}}.\nabla \mathrm{C} \tag{5}$$

Where C is the concentration of the solutions, R is the reaction rate, and D is the diffusion coefficient of the solutions. Since there is no reaction, R is zero [10] . By solving the three equations of continuity, momentum, and electric field, the velocity and pressure fields are obtained. The velocity field is placed in the convection-diffusion equation to describe the mass transfer in the micromixer and to obtain the desired unknowns.

Finally, the mixing efficiency is calculated using the following relation [34, 35]:

$$\mathrm{ME} = \left(1 - \frac{\int_0^{\mathrm{h}} |\mathrm{C} - \mathrm{C}_\infty| \mathrm{dy}}{\int_0^{\mathrm{h}} |\mathrm{C_o} - \mathrm{C}_\infty| \mathrm{dy}}\right) \times 100 \tag{6}$$

Where $C_\infty = (C_1 + C_2)/2$ is the average concentration and C_o is the initial concentration, which is zero for water and one for another fluid. C is the local concentration. The values of the other parameters are presented in Table 3. The values of fluid relative permittivity, molecular diffusivity, and zeta potential are selected based on previous papers [23, 32]. Other parameters, including frequency, inlet velocity, and potential are considered as a range to evaluate their impact on the performance of the micromixer.

Numerical method and Grid-Independence test

The finite element method and the commercial software COMSOL Multiphysics 5.5a are used to simulate the electroosmotic micromixer. The Navier-Stokes equations and electric equations are coupled to perform unsteady simulations using linear solver MUMPS. Also, the P2+P1 scheme is utilized to discretize the velocity and pressure.

One of the important parameters in numerical simulations is choosing an appropriate grid resolution because the number of elements affects the results and

Table 3: The value of parameters employed in the simulations.

Relative permittivity of the fluid	ε	80.2
Frequency, Hz	f	0.5-16
Temperature, ℃	T	25
Mean inflow velocity, mm/s	U_{in}	0.05-0.2
Molecular diffusion coefficient, m^2/s	D	10×10^{-11}
Electrical potential, V	V	0.05-0.5
Zeta potential, V	ξ_0	-0.1

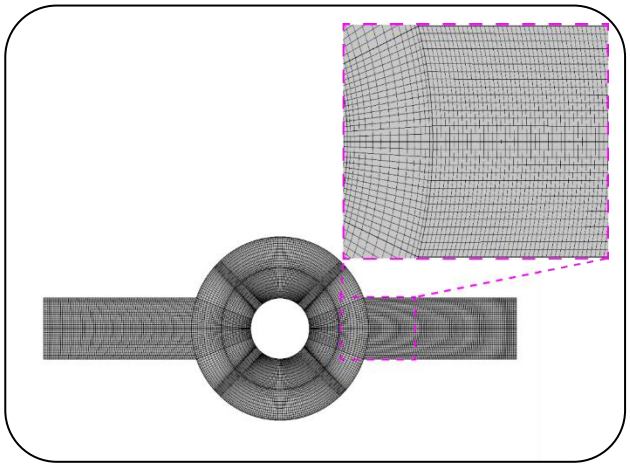

Fig. 2: The schematic of the grid used for the simulations.

solution time significantly. Structured rectangular meshes are employed to discretize the computational domain (Fig. 2). This type of mesh reduces the solution time compared to unstructured meshes. It should be noted that to reduce chemical damage before drug delivery, the mixing time is assumed to be 0.5 s because organic molecules are very fragile and their tolerance in the environment is less than one second.

In the micromixing of fluids, velocity distribution and species concentration are two sensitive parameters [36]. Thus, these two parameters are examined using different grid resolutions when a = 5 μm, V = 0.1 V, θ = 45°, and U_{in} = 0.05 mm/s. Fig. 3 illustrates the velocity profile at the microchannel outlet. When the number of grid points is low, there are some sharp velocity variations, and a parabolic velocity profile is obtained as the number of elements increases. Fig. 4 also shows the fluid concentration at the microchannel outlet. According to this figure, it can be seen that the number of elements strongly affects the mixing index of the two liquids. Figs. 3 and 4 the demonstrate that when the number of elements varies from 47878 to 90224, there is no difference between the results, and therefore the grid resolution of 47878 is selected for further simulations.

Validation

To verify the present simulations, the results of the present work are compared with the results reported by *Shamloo et al.* [32] who examined a two-ring electroosmotic micromixer in the presence of an AC electric field (Fig. 5). It is observed that the results obtained from the mixing efficiency and concentration distribution are in excellent agreement with their work, indicating that the simulation method leads to precise results. It should be pointed out that the values of ME are calculated at the micromixer outlet at different times.

RESULTS AND DISCUSSION

In the present study, liquid micromixing in an electroosmotic mixer in which electrodes are inserted into a mixing chamber is numerically simulated. This study aims to evaluate the influence of inlet velocity, height, and angle of the electrodes, voltage, and frequency.

Effect of inlet velocity

Fig. 6 shows the effect of inlet flow rate on the mixing of two liquids at the microchannel outlet for v = 0.1 V, *f* = 8 Hz, and a = 5 μm during 5 s. The figure demonstrates that increasing the inlet velocity from 0.1 to 0.2 mm/s reduces the mixing efficiency. However, when the inlet velocity is enhanced from 0.05 to 0.1 mm/s, the mixing quality is improved. In other words, there is an optimum point for the inlet velocity. At t = 0.5 s, the mixing efficiency for U_{in} = 0.05, 0.1, 0.15, and 0.2 mm/s is 85.97, 93.66, 91.19, 87%, respectively. When the fluid velocity

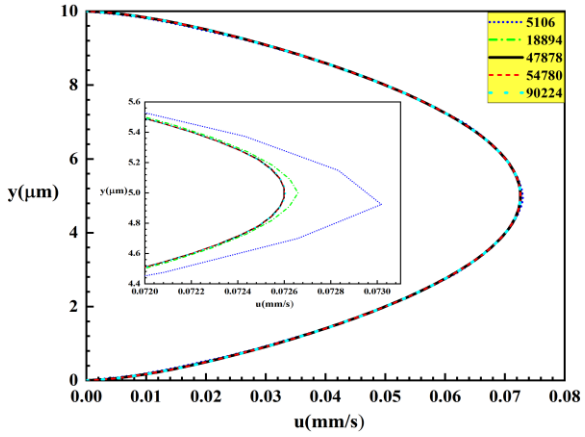

Fig. 3: Velocity distribution at the microchannel outlet for different grid resolutions.

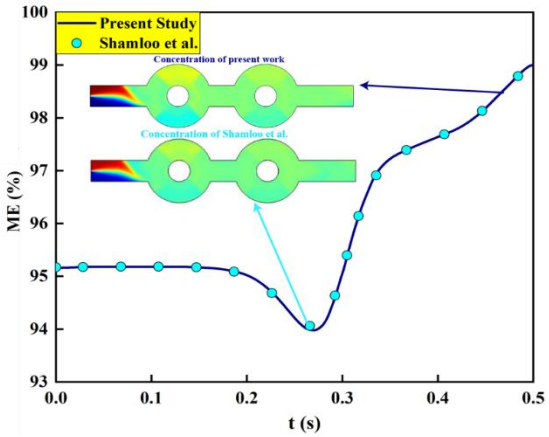

Fig. 5: Mixing efficiency and concentration distribution for U_{in} = 0.05 mm/s V, f = 4 Hz, and v = 0.5 V.

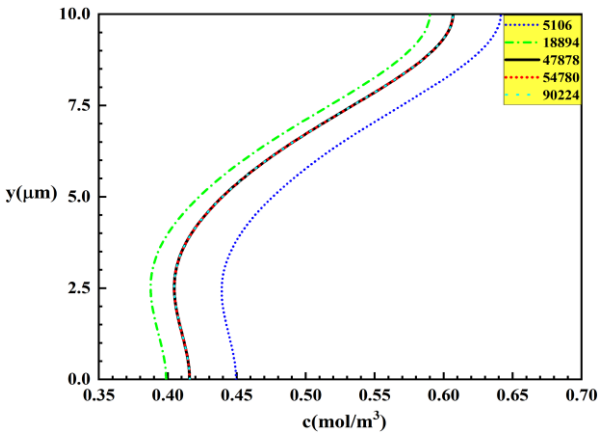

Fig. 4: Concentration distribution at the microchannel outlet for different grid resolutions.

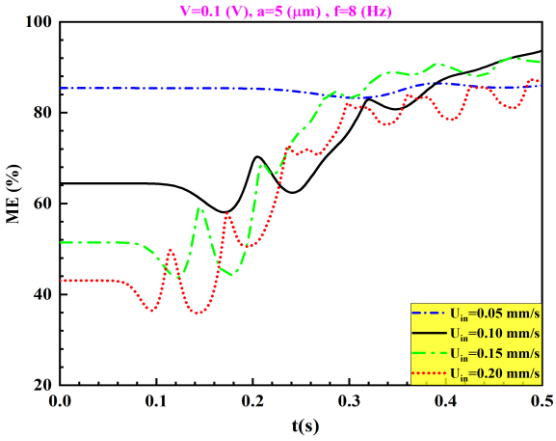

Fig. 6. Mixing efficiency versus time for different inlet velocities.

is low, molecular diffusion has a significant effect on the mixing of the two liquids. Since fluid momentum increases with the velocity, the mixing due to molecular diffusion decreases by increasing the flow rate. However, the existence of the optimum point indicates that there is a competition between inertia and electroosmotic forces. It can be concluded that the optimum value for inlet velocity is expected for all electroosmotic micromixers, depending on other effective parameters such as mixer geometry, voltage, frequency, etc. Fig. 7 shows the concentration contours for different inlet velocities and reveals that inlet velocity affects the formation of vortices. At U_{in} = 0.05 and 0.1 mm/s, the number of vortices is higher than the two other cases. It should be pointed out that the liquids with an inlet velocity of 0.05 mm/s require a larger mixing time compared to other flow rates. Hence, mixing quality is slightly changed with the time (Fig. 6).

Effect of electrode height

The effect of electrode height on the mixing of two liquids is shown in Fig. 8. The height of the electrodes varies from zero (when the electrodes are attached to the mixing chamber surface) to 7.5 μm. The results show that when the electrode height has a positive effect on the mixing efficiency. This is due to the formation of more vortices when electrodes play the role of obstacles. Fig. 9 reveals that when the electrodes are attached to the microchannel wall, six small vortices are formed around the inner cylinder. As the electrodes enter the microchannel, two more vortices are formed in the space

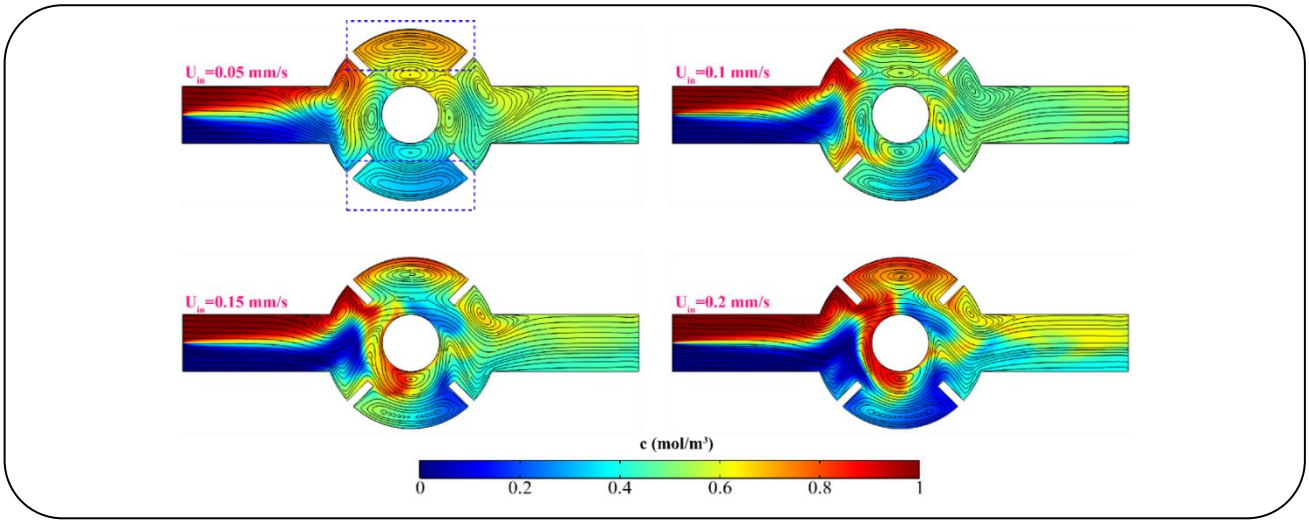

Fig. 7: Concentration distribution inside the micromixer for different inlet velocities.

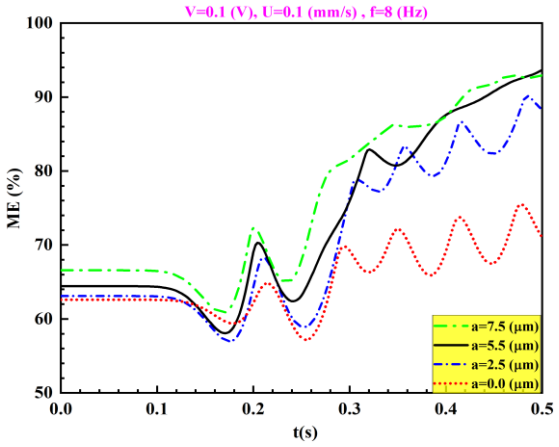

Fig. 8: Mixing efficiency in terms of electrode height.

between the two electrodes. In other words, a strong vortex and a weak one are created between two electrodes due to the combined effect of the electric field and obstacle. Since these electrodes act as obstacles, the flow turbulence inside the mixing chamber is enhanced, leading to an increase in the mixing degree. In other words, when the height of the electrodes increases, two positive effects occur. First, the contact surface between the electrodes and liquids increases with the electrode height, and more amounts of liquids are subjected to electrokinetic force. Second, the electrode causes more turbulence inside the micromixer. According to the data obtained at t = 0.5 s, the maximum mixing efficiency is obtained when the height of the electrodes is 5 μm. As the electrode height varies from 0 to 5 μm, the mixing index increases from 71.01% to 93.66%. It should be noted that when the height of the electrode changes from 0 to 2.5 μm, the mixing efficiency increases by 24%, and when it varies from 2.5 to 5 μm, the mixing index increases by 6.1%, indicating that the mixing efficiency decreases with the electrode height eventually.

Effect of the electrode angle

Fig. 10 illustrates the mixing efficiency versus time for a = 5 μm, U_{in} = 0.1 mm/s, and different electrode angles during 0.5 s. The results show that there is an optimum value for the electrode angle (θ = 60°) in which the maximum amount of mixing efficiency of 94.92% is obtained. For electrode angle of 0°, the mixing index is minimum, i.e. 82.79%, indicating that the angle of the electrodes can increase the mixing efficiency by 14%. It should be noted that the difference between mixing efficiency for θ = 45° and 60° is less than 1%. Fig. 11 shows the concentration contours and streamlines for different electrode angles. This figure qualitatively confirms that the mixing index is enhanced when the electrode angle increases. When θ = 60°, the vortex formed between two electrodes is larger and stronger than the other angles. As the electrode angle varies from 60° to 75°, this vortex tends to be divided into two small vortices, leading to the creation of lower turbulence and lower mixing efficiency.

Effect of voltage

One of the most important factors affecting the mixing of two liquids is the voltage of the electrodes. Fig. 12 shows

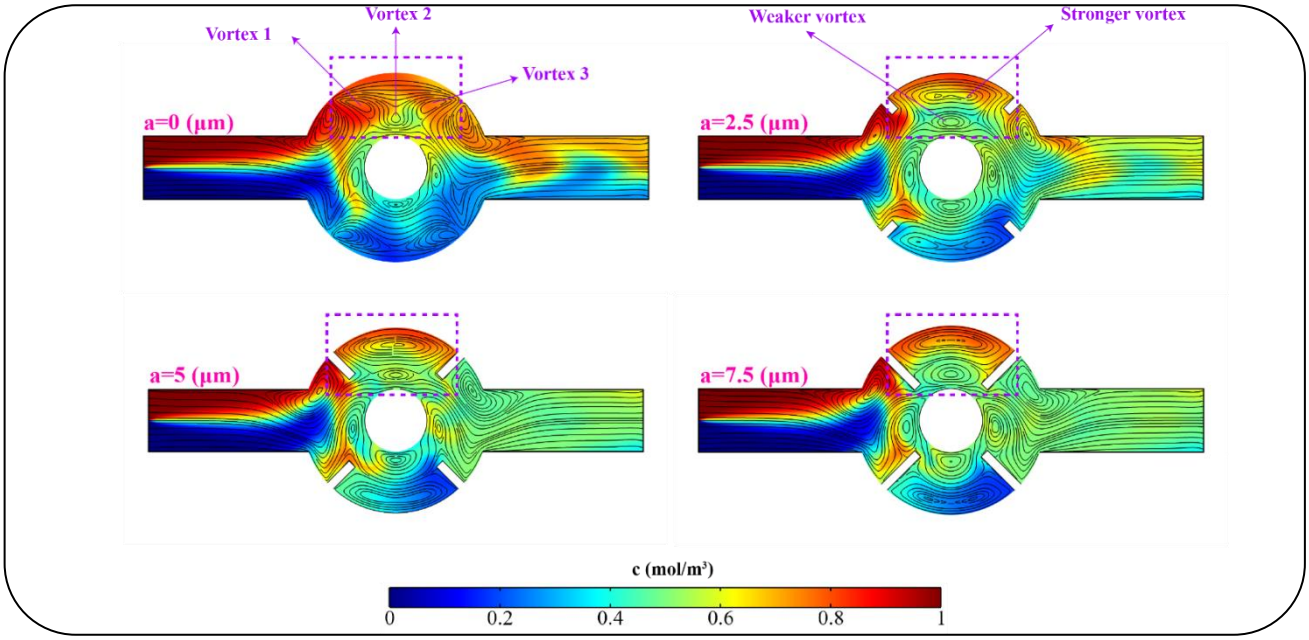

Fig. 9: Concentrations distribution inside the micromixer for different electrode heights.

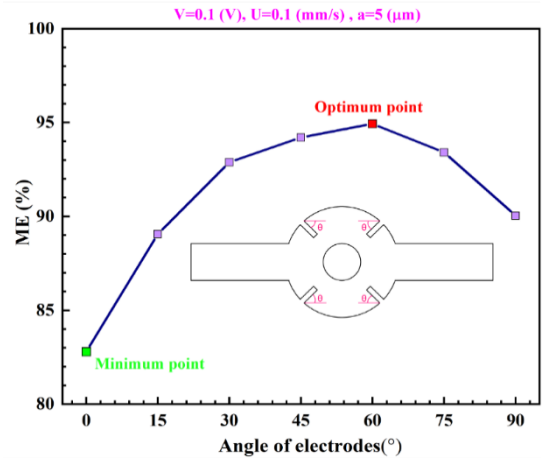

Fig. 10: Mixing efficiency in terms of time for different electrode angles.

the variations of mixing efficiency for θ = 60°, a = 5 μm, U_{in} = 0.1 mm/s and different voltages during 0.5 s. This figure qualitatively shows that the mixing index increases significantly by increasing the voltage. Previous sections proved that the formation of vortices is the most important parameter that affects the mixing quality in an electroosmotic micromixer. The voltage can increase or decrease the mixing index by controlling these vortices. As shown in Fig. 12, when the voltage changes from 0.05 V to 0.5, the number of vortices is increased. It can be seen that when the voltage is 0.05 V, there is only a single vortex between pair of electrodes and as the voltage increases, the second vortex is formed close to the first one. This area is marked with a dashed line in the figure. In other words, as the voltage increases, the electro-osmotic forces overcome the inertia force, increasing mass diffusion in the liquid-liquid interface.

Fig. 13 shows that there are the most fluctuations in the mixing efficiency curve versus time when v = 0.05 V. The fluctuations decrease with increasing the voltage, indicating that the mixing process occurs in less time at higher voltages. At t = 0.46, the mixing index for the two voltages of 0.2 and 0.5 V becomes constant, while for the other two cases it is still changing. As the voltage changes from 0.05 to 0.5 V, the mixing efficiency increases from 83.72 to 98.7%. It should be noted that when the voltage varies from 0.2 to 0.5 V, the mixing changes from 97.66 to 98.70%, showing that the mixing efficiency increases by only 1%. It is expected that a further increase in the voltage has a slight effect on mixing improvement.

Effect of frequency

Since AC frequencies are employed in the present work, the mixing efficiency is calculated for θ= 60°, a= 5 μm, U_{in}= 0.1 mm/s, v= 0.1 V, and different frequencies during 0.5 s (Fig. 14). Although it is expected that mixing efficiency is increased with the AC frequency [11, 20], the present results show that there is an optimal frequency

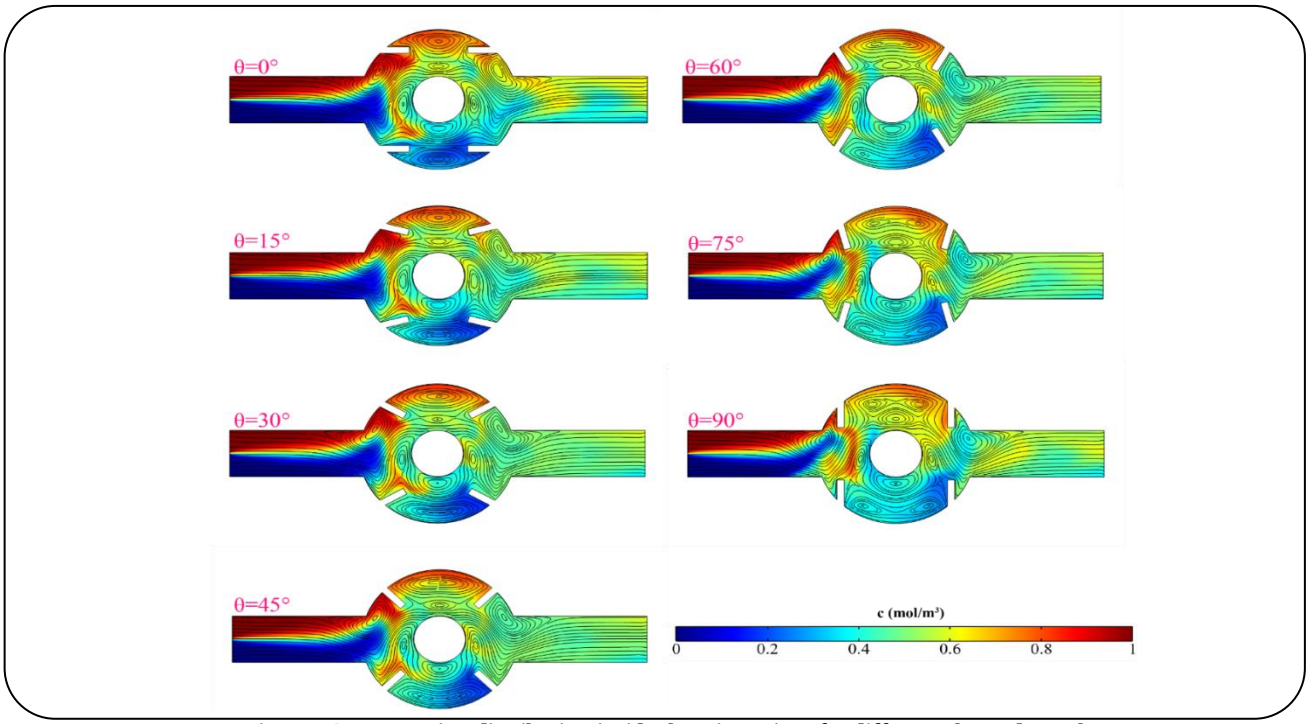

Fig. 11: Concentration distribution inside the micromixer for different electrode angles.

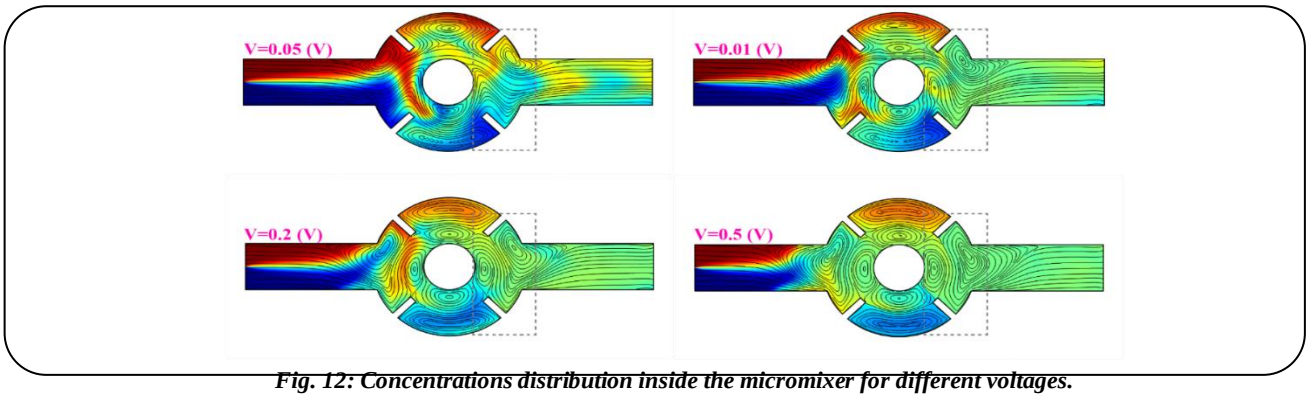

Fig. 12: Concentrations distribution inside the micromixer for different voltages.

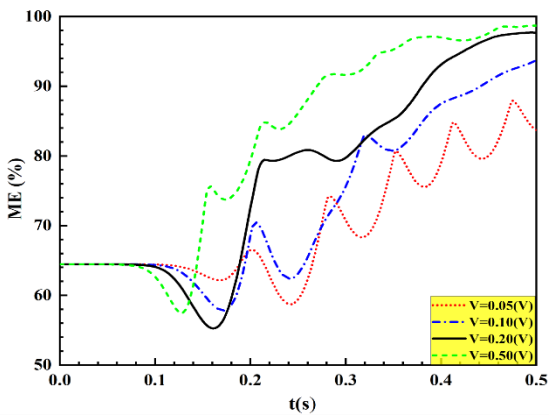

Fig. 13: Mixing efficiency in terms of time for different voltages.

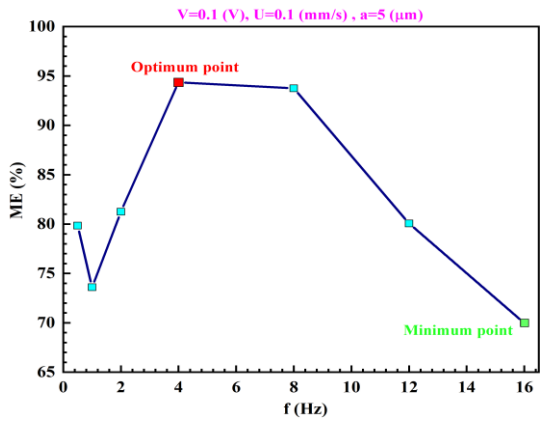

Fig. 14: Mixing efficiency in terms of time for different AC frequencies.

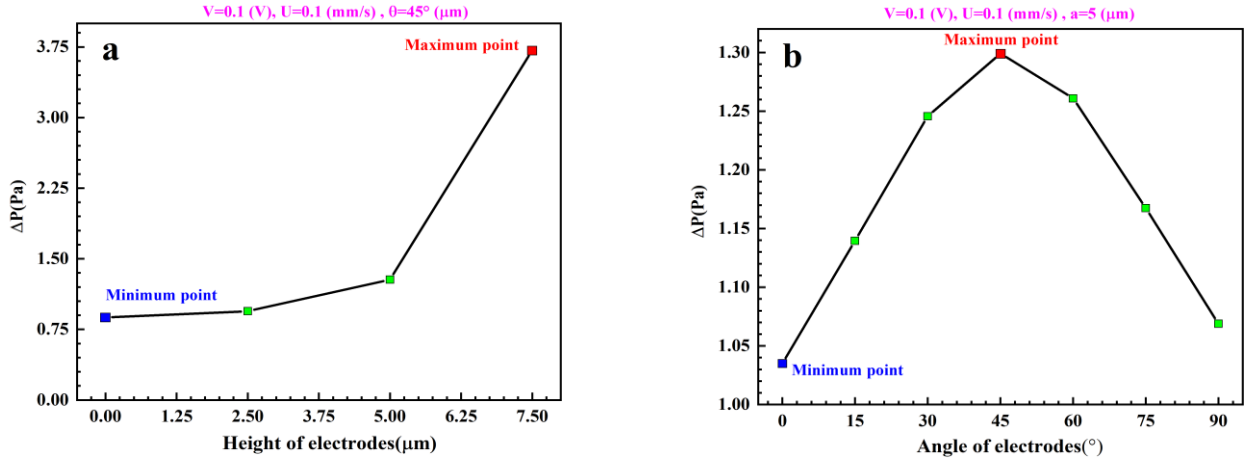

Fig. 15: Pressure drop in terms of (a) electrode height and (b) electrode angle.

in which the maximum mixing efficiency is reached. The minimum mixing quality is observed for the frequency of 16 Hz and the maximum one corresponds to f = 4 Hz. As can be seen, the mixing index increases with a very sharp slope while the frequency increases from 0.5 to 4 Hz and decreases from 8 to 16 Hz.

Pressure drop and performance coefficient

When the electrodes enter the chamber, although they increase the mixing degree of the liquids, it also affects the pressure drop of the micromixer. In this section, the pressure drop is also examined when the height and angle of electrodes vary from 0 to 7.5 μm and 0 to 90°, respectively. Fig. 15a shows that the pressure drop increases with increasing the electrode height. When the height of the electrodes increases, the blockage effect is enhanced, making the liquid passage smaller. Thus, the pressure drop increases with the electrode height. As the height of the electrodes changes from 0 to 2 μm, the pressure drop increases by 8.04%, while it increases by 143.73% when the height of the electrodes varies from 2.5 to 5 μm. Fig. 15b shows the effect of the electrode angle on the pressure drop. It can be seen that the minimum pressure drop is related to θ = 0°. Since the electrodes are not directly placed in the liquid path when θ = 0°, the blockage effect is small and the pressure drop is minimal The maximum value of pressure drop corresponds to θ = 45°. The electrodes with this angle disturb the liquids more, resulting in a greater pressure drop. Fig. 16 reveals that the fluid velocity between the inner cylinder and the electrodes (highlighted area) for θ = 0° is lower than that for other electrodes angles. The velocity in this region for θ = 45° is higher than that for other angles. This is due to the blockage effect and a reduction in the liquid passage. According to Bernoulli's equation, a reduction in the velocity increases the pressure drop.

Previous results demonstrate that the mixing efficiency and pressure drop increase with the electrode height. Hence, the presence of electrodes with a ≠ 0 leads to a positive and a negative effect on micromixer performance. Therefore, in this section, the performance of the mixer is evaluated by considering these two effects. Figs. 17 a and b show the performance of the micromixer with different heights and angles of electrodes, respectively, relative to the base micromixer in which a = 0 μm. It can be observed that the pressure drop ratio, $\Delta p/\Delta p_{base}$ is greater than the mixing efficiency ratio ME/ME_{base}. Fig. 17a demonstrates that the rate of an increase in the mixing efficiency of the micromixer is smaller than the rate of enhancement in the pressure drop when electrode height is increased. As expected, the presence of an obstacle in the mixing chamber results in an increase in the pressure drop and mixing index simultaneously. The figure shows the proposed micromixer has a better performance than the base one when a = 2.5 μm.

As mentioned before, increasing the height of the electrode and changing the angle of the electrode have a positive effect and a negative one. To consider the positive and the negative effect simultaneously, the following definition is employed:

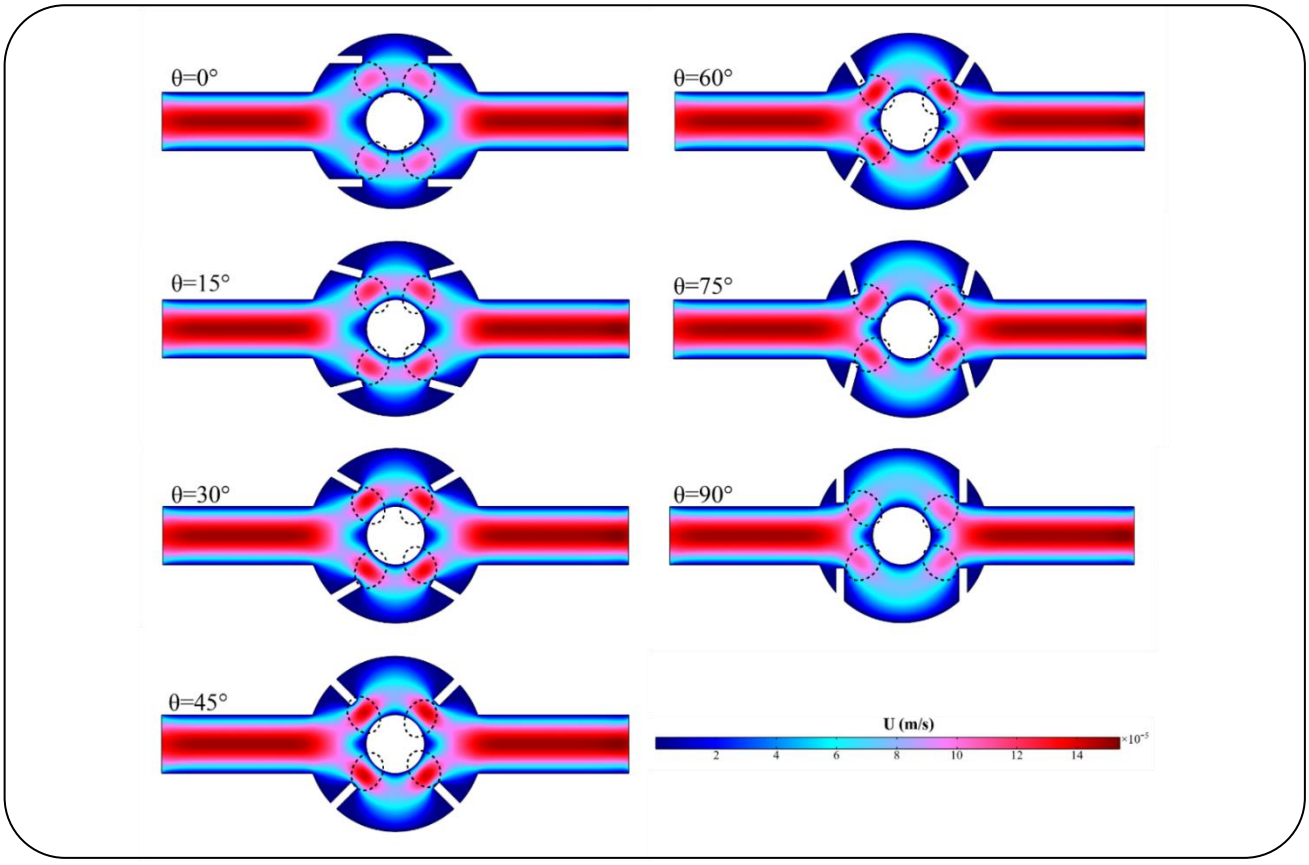

Fig. 16: Fluid velocity distribution for different electrode angles.

$$\mathrm{COP} = \frac{\dfrac{\mathrm{ME}}{\text{Pressure drop}}}{\dfrac{\mathrm{ME}_{\mathrm{base}}}{\text{Pressure drop}_{\mathrm{base}}}} \qquad (7)$$

According to this relation, if this number is more than one, the efficiency of the positive effect is larger than the negative one and the micromixer can be suggested as an efficient mixer in comparison with the reference geometry. In Figs. 18 a and b, the value of COP is plotted for different heights and angles of electrodes, respectively. This figure shows that at a height of 2.5 μm, the COP is more than one, i.e. COP = 1.15. Also, the minimum COP is related to a = 7.5 μm and its value is equal to 0.3. On the other hand, although the maximum mixing is obtained at θ = 60°, the COP is 0.89. At θ = 90°, the COP is higher than one, i.e. COP = 1.21.

CONCLUSIONS

In the present work, an electroosmotic micromixer whose electrodes enter the mixing chamber is simulated to evaluate the effect of inlet velocity, voltage, frequency, angle, and height of the electrodes on mixing quality and pressure drop. The proposed micromixer can be utilized in the field of chemistry and biochemistry. The results demonstrate that the maximum mixing index, i.e. 94.92%, corresponds to θ = 60°. The optimal value for electrode height, i.e. a = 5 μm, is obtained. When the height of the electrodes changes from 0 to 2.5 μm, the mixing quality is improved by 24%, while as the height of the electrode varies 2.5 to 5 μm, the improvement is 6.1%. The results show that increasing the voltage always enhances the mixing efficiency and a frequency of 4 Hz is an optimal value in which the mixing efficiency reaches 94.36%. Micromixer performance is evaluated by defining the COP and the calculations show that the COP is more than one for a = 2.5 μm and θ = 90°. Finally, some suggestions are provided for future investigations: (i) evaluation of the impact of other geometries for the mixing chamber such as square and diamond in the presence of fin-shaped electrodes, (ii) study of the influence of proposed

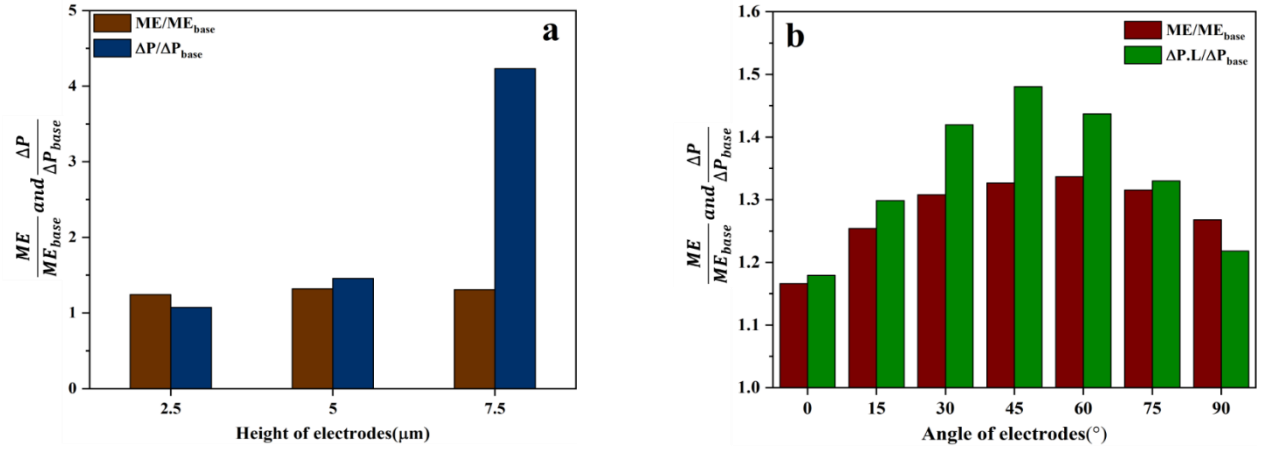

Fig. 17: Investigation of pressure drop and mixing efficiency for different heights and angles of electrodes compared to the reference case.

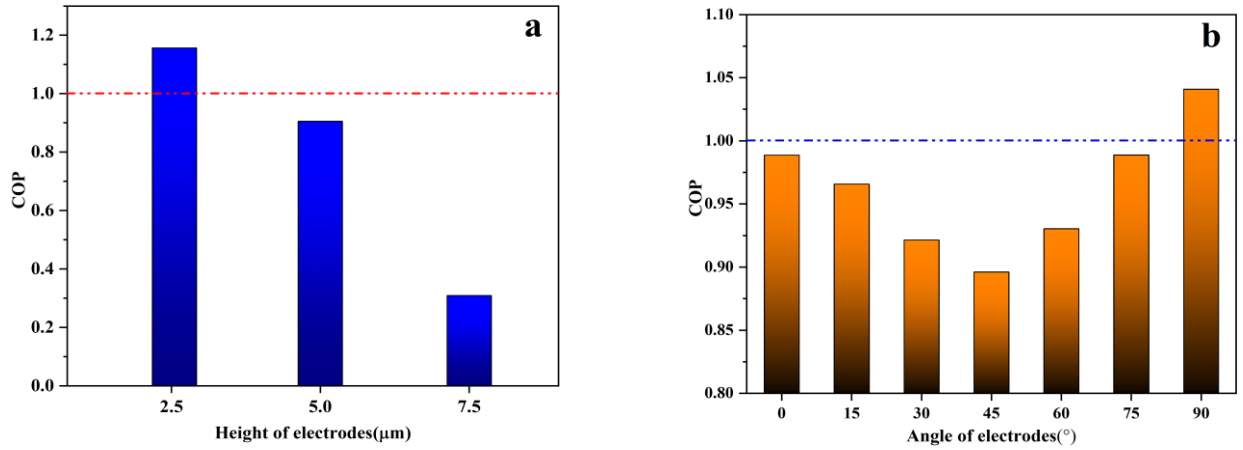

Fig. 18: The COP of the micromixer for different heights and angles of electrodes compared to the reference case.

electroosmotic micromixer for shear-thinning, shear-thickening, and viscoelastic fluids, and (iii) using an external heat source by placing a film heater at the bottom of the mixing chamber to evaluate the mixing of conductive fluids.

Received : Dec. 8, 2021 ; Accepted : Feb. 14, 2022

REFERENCES

[1] Bahrami D., Nadooshan A. A., Bayareh M., Numerical Study on The Effect of Planar Normal and Halbach Magnet Arrays on Micromixing, *International Journal of Chemical Reactor Engineering*, **18**, (2020).

[2] Bayareh M., Ghasemi B., Nazemi Ashani M., Acoustofluidic Separation of Microparticles: A Numerical Study, *Iranian Journal of Chemistry and Chemical Engineering (IJCCE)*,**41(9):** 2873-2886 (2021).

[3] Bayareh M., Ashani M. N., Usefian A., Active and Passive Micromixers: A Comprehensive Review, *Chemical Engineering and Processing-Process Intensification*, **147**: 107771 (2020).

[4] Lee C.-Y., Fu L.-M., Recent Advances and Applications of Micromixers, *Sensors and Actuators B: Chemical*, **259**: 677-702 (2018).

[5] Hadjigeorgiou A. G., Boudouvis A. G., Kokkoris G., Thorough Computational Analysis of the Staggered Herringbone Micromixer Reveals Transport Mechanisms and Enables Mixing Efficiency-Based Improved Design, *Chemical Engineering Journal*, **414**: 128775 (2021).

[6] Chen X., Li T ,.Zeng H., Hu Z., Fu B., Numerical and Experimental Investigation on Micromixers with Serpentine Microchannels, *International Journal of Heat and Mass Transfer*, **98**: 131-140 (2016).

[7] Babaie Z., Bahrami D., Bayareh M., Investigation of a Novel Serpentine Micromixer Based on Dean Flow and Separation Vortices, *Meccanica, 57:* 73-86 (2022).

[8] Chen X., Li T., A Novel Passive Micromixer Designed by Applying an Optimization Algorithm to the Zigzag Microchannel, *Chemical Engineering Journal*, **313**: 1406-1414 (2017).

[9] Bahrami D., Bayareh M., Impacts of Channel Wall Twisting on the Mixing Enhancement of a Novel Spiral Micromixer, *Chemical Papers*, 1-12 (2021).

[10] Bahrami D., Bayareh M., Experimental and Numerical Investigation of a Novel Spiral Micromixer with Sinusoidal Channel Walls, *Chemical Engineering & Technology*, **45**: 100-109 (2022).

[11] Hejazian M., Nguyen N.-T., A Rapid Magnetofluidic Micromixer Using Diluted Ferrofluid, *Micromachines*, **8**: 37 (2017).

[12] Lim E., Lee L., Yeo L. Y., Hung Y. M., Tan M. K., Acoustically Driven Micromixing: Effect of Transducer Geometry, *IEEE Transactions on Ultrasonics, Ferroelectrics, and Frequency Control*, **66**: 1387-1394 (2019).

[13] Lv H., Chen X., New Insights into the Mechanism of Fluid Mixing in the Micromixer Based on Alternating Current Electric Heating with Film Heaters, *International Journal of Heat and Mass Transfer*, **181**: 121902 (2021).

[14] Ding H., Zhong X., Liu B., Shi L ,.Zhou T., Zhu Y., Mixing Mechanism of a Straight Channel Micromixer Based on Light-Actuated Oscillating Electroosmosis in Low-Frequency Sinusoidal AC Electric Field, *Microfluidics and Nanofluidics*, **25**: 1-15 (2021).

[15] Afzal A., Kim K-.Y., "Analysis and Design Optimization of Micromixers", Springer, pp. 11-34 (2021).

[16] Rashidi S., Bafekr H., Valipour M.S., Esfahani J.A., A Review on the Application, Simulation, and Experiment of the Electrokinetic Mixers, *Chemical Engineering and Processing-Process Intensification*, **126**: 108-122 (2018).

[17] Nayak A., Analysis of Mixing for Electroosmotic Flow in Micro/Nano Channels with Heterogeneous Surface Potential, *International Journal of Heat and Mass Transfer*, **75**: 135-144 (2014).

[18] Banerjee A., Nayak A., Haque A., Weigand B., Induced Mixing Electrokinetics in a Charged Corrugated Nano-Channel: Towards a Controlled Ionic Transport, *Microfluidics and Nanofluidics*, **22**: 1-21 (2018).

[19] Nayak A., Haque A., Weigand B., Wereley S., Thermokinetic Transport of Dilatant/Pseudoplastic Fluids in a Hydrophobic Patterned Micro-Slit, *Physics of Fluids*, **32**: 072002 (2020).

[20] Haque A., Nayak A., Bhattacharyya S., Numerical Study on Ion Transport and Electro-Convective Mixing of Power-Law Fluid in a Heterogeneous Micro-Constrained Channel, *Physics of Fluids*, **33**: 122014 (2021).

[21] Khakpour A., Ramiar A., Numerical Investigation of the Effect of Electrode Arrangement and Geometry on Electrothermal Fluid Flow Pumping and Mixing in Microchannel, *Chemical Engineering and Processing-Process Intensification*, **150**: 107864 (2020).

[22] Seo H.-S., Han B., Kim Y.-J., Numerical Study on the Mixing Performance of a Ring-Type Electroosmotic Micromixer with Different Obstacle Configurations, *Journal of Nanoscience and Nanotechnology*, **12**: 4523-4530 (2012).

[23] Usefian A., Bayareh M., Shateri A., Taheri N., Numerical Study of Electro-Osmotic Micro-Mixing of Newtonian and Non-Newtonian Fluids, *Journal of the Brazilian Society of Mechanical Sciences and Engineering*, **41**: 1-10 (2019).

[24] Basati Y., Mohammadipour O. R., Niazmand H., Numerical Investigation and Simultaneous Optimization of Geometry and Zeta-Potential in Electroosmotic Mixing Flows, *International Journal of Heat and Mass Transfer*, **133**: 786-799 (2019).

[25] Zhang K., Ren Y., Hou L., Feng X., Chen X., Jiang H., An Efficient Micromixer Actuated by Induced-Charge Electroosmosis Using Asymmetrical Floating Electrodes, *Microfluidics and Nanofluidics*, **22**: 1-11 (2018).

[26] Alipanah M., Ramiar A., High Efficiency Micromixing Technique Using Periodic Induced Charge Electroosmotic Flow: A Numerical Study, *Colloids and Surfaces A: Physicochemical and Engineering Aspects*, **524**: 53-65 (2017).

[27] Usefian A., Bayareh M., Numerical and Experimental Study on Mixing Performance of a Novel Electro-Osmotic Micro-Mixer, *Meccanica*, **54**: 1149-1162 (2019).

[28] Hadigol M., Nosrati R., Nourbakhsh A., Raisee M., Numerical Study of Electroosmotic Micromixing of Non-Newtonian Fluids, *Journal of Non-Newtonian Fluid Mechanics*, **166**: 965-971 (2011).

[29] Jalili H., Raad M., Fallah D. A., Numerical Study on the Mixing Quality of an Electroosmotic Micromixer under Periodic Potential, *Proceedings of the Institution of Mechanical Engineers, Part C: Journal of Mechanical Engineering Science*, **234**: 2113-2125 (2020).

[30] Cheng Y., Jiang Y., Wang W., Numerical Simulation for Electro-Osmotic Mixing under Three Types of Periodic Potentials in a T-Shaped Micro-Mixer, *Chemical Engineering and Processing-Process Intensification*, **127**: 93-102 (2018).

[31] Zhou T., Wang H., Shi L., Liu Z., Joo S.W., An Enhanced Electroosmotic Micromixer with an Efficient Asymmetric Lateral Structure, *Micromachines*, **7**: 218 (2016).

[32] Shamloo A., Mirzakhanloo M., Dabirzadeh M.R., Numerical Simulation for Efficient Mixing of Newtonian and Non-Newtonian Fluids in an Electro-Osmotic Micro-Mixer, *Chemical Engineering and Processing-Process Intensification*, **107**: 11-20 (2016).

[33] Chen X., Wu Z., Design and Numerical Simulation of a Novel Microfluidic Electroosmotic Micromixer with Three Electrode Pairs, *Journal of Chemical Technology & Biotechnology*, **94**: 1991-1997 (2019).

[34] Basati Y., Mohammadipour O.R., Niazmand H., Design and Analysis of an Electroosmotic Micro-Reactor and its Application on Controlling a Chemical Reaction, *Chemical Engineering and Processing-Process Intensification*, **164**: 108381 (2021).

[35] Bahrami D., Nadooshan A. A., Bayareh M., Effect of Non-Uniform Magnetic Field on Mixing Index of a Sinusoidal Micromixer, *Korean Journal of Chemical Engineering*, (2022).

[36] Bayareh M., Artificial Diffusion in the Simulation of Micromixers: A Review, *Proceedings of the Institution of Mechanical Engineers, Part C: Journal of Mechanical Engineering Science*, **253**: 5288-5296 (2021).